Dynamics of a driven two-level atom coupled to a frequency-tunable cavity

Peng Zhou* and S. Swain†
Department of Applied Mathematics and Theoretical Physics, The Queen's University of Belfast, Belfast BT7 1NN, Northern Ireland, United Kingdom

(Received 5 September 1997; revised manuscript received 18 February 1998)

A cavity-modified master equation is derived for a coherently driven two-level atom coupled to a single-mode cavity in the bad cavity limit, in which the cavity frequency is tuned to either the center or one of the sidebands of the Mollow triplet. The atomic populations in both the bare- and dressed-state representations are analyzed in terms of the cavity-modified transition rates. In the bare-state basis, the role of the cavity may be interpreted as enhancing the stimulated absorption of the atom while suppressing the stimulated emission. The bare-state population may thus be inverted under appropriate conditions. The dressed-state inversion, however, originates from the enhancement of the atom-cavity interaction when the cavity is resonant with the atomic dressed-state transition. We show that two-phase quadratures of the atomic polarization decay at different rates. The decay of the in-phase (or out-of-phase) quadrature may be greatly inhibited as the driving intensity increases, depending on the cavity resonant frequency. The spectrum of the atomic fluorescence emitted out the side of the cavity is also studied. The spectral profiles are sensitive to the cavity frequency. When the cavity frequency is tuned to the center of the Mollow resonances, the fluorescence spectrum is symmetrical with three peaks whose linewidths and heights are intensity dependent. When the cavity frequency is tuned to one of the Mollow sidebands, however, it is asymmetric, and the central peak and the sideband on resonance with the cavity can be significantly suppressed for strong driving fields. All three spectral lines can be narrowed by increasing the Rabi frequency. The physics of these striking spectral features is explored in the dressed-state basis. We also investigate the probe absorption spectrum. When the cavity frequency is tuned to the center of the Mollow fluorescence triplet, the central component exhibits a Lorentzian line shape, while the side bands show the Rayleigh-wing line shape. Probe gain may occur at line center due to cavity-induced, bare-state population inversion. When the cavity is tuned to resonance with one sideband, only two sidebands, with Lorentzian profiles, dominate. Gain can occur at the sideband far off resonant with the cavity. The sideband gain is a consequence of an unbalanced dressed-state population distribution. [S1050-2947(98)07706-3]

PACS number(s): 42.50.Ct, 42.50.Hz, 42.50.Dv

I. INTRODUCTION

A fundamental model for light-matter interactions in quantum optics and laser physics is that of an excited, two-level atom interacting with the infinite number of electromagnetic modes of the vacuum in free space. The radiative properties of this system are well understood: an exponential rate of decay to the ground level, giving rise to a Lorentzian spectrum with the natural linewidth. In the presence of a strong laser beam, however, novel radiative effects can dominate, since the excited atom can be stimulated to emit and absorb several photons from the driving field during the time interval for one spontaneous decay. The decay of the excited state is thus modulated with oscillations at the Rabi frequency. Consequently, the fluorescence spectrum develops into the Mollow triplet [1,2] , in which the sidebands are symmetrically shifted from the laser frequency ω_L by the generalized Rabi frequency $\overline{\Omega}$, and are one and a half times as wide and one-third as high as the central peak. The widths and heights of the triplet are independent of the intensity of the laser field. The characteristic symmetric triplet structure can also be inferred from a dressed-state model [3].

The probe absorption spectrum of such a driven atom also exhibits a triplet structure in high driving intensities [4–6]. The spectral features, however, depend on the detuning of the atom from the driving field. For resonant excitation, the central component has a Lorentzian line shape, while the Rabi sidebands exhibit dispersionlike (Rayleigh-wing type) profiles [4,5]. However, when the driving field is detuned from resonance with the atomic transition frequency, the central resonance of the absorption spectrum exhibits a dispersion-like profile, while the sidebands are two Lorentzians in which one shows absorption of the probe beam and the other amplification [5,6].

Over the past decade, considerable interest has been devoted to systems in which atoms interact with a modified vacuum, such as that presented by a cavity [7], where the electromagnetic modes are concentrated around the cavity resonant frequency. The coupling of the atoms to the modified electromagnetic vacuum is therefore frequency dependent. For an excited atom located inside such a cavity, the cavity mode is the only one available to the atom for emission. If the atomic transition is in resonance with the cavity, the spontaneous emission rate into the particular cavity mode is enhanced [8]; otherwise, it is inhibited [9]. Therefore, one may manipulate the atomic decay rate by tuning the cavity into or out of resonance with the radiative atom. Cavity-enhanced and cavity-inhibited spontaneous emission, resulting in a broadening or narrowing of the spectrum, has been

*Electronic mail: peng@qo1.am.qub.ac.uk
†Electronic mail: s.swain@qub.ac.uk

observed by several groups [8,9]. On the other hand, when the atom-cavity coupling is very strong, the spontaneously emitted photon may be repeatedly absorbed and emitted by the atom before it leaves the cavity. This effect results in an oscillatory exchange of energy between the atom and the cavity field, which in turn leads to a splitting of the spontaneous emission spectrum. Such a splitting, termed ''vacuum Rabi splitting,'' has been widely investigated both theoretically and experimentally [10].

Atomic radiative properties can be modified not only by the essentially passive means described above, but also through dynamical means, i.e., by imposing a coherent driving field on the atoms. Rice and Carmichael [11] showed that for a system with a large cavity decay rate with weak atom-cavity coupling, a weakly driven atom inside the cavity behaves formally the same as in free space, but with a renormalized decay rate. A fully quantum mechanical analysis of the system by Savage, however, predicted a steady-state atomic population inversion due to its coupling to the cavity [12]. Recently, Lewenstein and co-workers [13] demonstrated that a strong driving field may dynamically suppress the rate of atomic spontaneous emission, and so dramatically modify the resonance fluorescence spectrum. The intense-field effect of the cavity-induced spontaneous emission was observed later in a microwave cavity [14], as well as in an optical cavity [15,16]. For strong atom-cavity coupling, Savage's study [17] showed that the resonance fluorescence spectrum has two sidebands with a linewidth given by the atom-cavity coupling constant rather than the system dissipation rate. Population inversion and multipeaked spontaneous emission spectra of a two-level atom coupled strongly to a cavity at a finite temperature were reported by Cirac, Ritsch, and Zoller [18]. Similar multipeaked spectral features have been shown to occur in a strongly coupled atom-cavity system in which the atom is subject to incoherent pumping [19].

Most studies mentioned above were carried out by assuming that the cavity is in resonance with the atomic transition and the driving laser. However, a series of investigations reported very recently by Freedhoff and Quang [20–22] showed a variety of remarkable effects when the cavity frequency is tuned to one of the sidebands of the Mollow spectrum. For instance, in the moderate atom-cavity coupling regime the steady-state atomic population may be highly inverted [20], and all the spectral components of the Mollow triplet become extremely narrow [21], whereas, for strong atom-cavity coupling, both the resonance fluorescence and probe absorption spectra split into multiplets whose structures depend on the photon-number distribution of the cavity field [22]. Recently, Zhu, Lezama, and Mossberg [15] reported an experimental study of the effects of cavity detuning on the atomic radiative properties. They showed that the atomic fluorescence of a strongly driven, off-resonant, two-level atom can be enhanced when the cavity frequency is tuned to one of the sidebands of the Mollow spectrum, whereas it can be inhibited by tuning to the other sideband. The enhancement of atomic fluorescence at one sideband is a direct demonstration of population inversion.

In this paper, we study the dynamical modification of the radiative properties of a coherently driven two-level atom coupled to a frequency-tunable, single-mode cavity in the bad cavity limit. The properties discussed include population inversion, transverse and longitudinal decay rates, resonance fluorescence, and probe absorption spectra. We consider the general case in which both the atom and cavity can be either on resonance or off resonance with the driving field. The bad cavity assumption permits one to obtain analytical expressions from which one may gain further insight into the modification of the atomic radiative properties by a cavity.

This paper is organized as follows. In Sec. II, we derive a cavity-modified master equation for the atomic density-matrix operator from the full master equation by adiabatically eliminating the cavity variables in the bad cavity limit. We find that the cavity-induced rate of spontaneous emission is strongly dependent on the atom-cavity coupling, Rabi frequency and cavity resonance frequency. In Sec. III, we discuss the atomic population dynamics in the bare-state basis in terms of the cavity-modified transition rates, and show that the cavity can enhance the stimulated absorption of the atom while suppressing the stimulated emission. The population may therefore be inverted for certain conditions. We explore the origin of the atomic population inversion in Sec. IV, by working in the dressed-state basis. The population inversion results from the cavity-enhanced interaction between the atom with the cavity when the atomic dressed-state transition is in resonance with the cavity. We study the intense-field cavity-modified relaxation rates of the atomic polarization and population in Sec. V, where we show that the two-phase quadrature components of the atomic polarization have different decay rates, as is the case in a squeezed vacuum [23], and that the cavity-induced decay into the cavity mode of the in-phase (or out-of-phase) quadrature can be completely suppressed for large Rabi frequencies, depending on the cavity frequency. In Sec. VI, we explore the resonance fluorescence spectrum for emission into the background modes. The features of the resonance fluorescence spectrum are displayed numerically and interpreted in the dressed-state basis. Section VII is devoted to the cavity-modified probe absorption spectrum. Amplification of the probe beam can take place at either the center or at one sideband, depending on the cavity resonant frequency. We present conclusions in Sec. VIII.

II. CAVITY-MODIFIED MASTER EQUATION

We consider a single two-level atom with transition frequency ω_A coupled to a single-mode cavity field of frequency ω_C. The atom is driven by a coherent laser field of frequency ω_L. The cavity mode is described by annihilation and creation operators a and $a^\dagger$, while the atom is represented by the usual Pauli spin-$\frac{1}{2}$ operators σ_+ and σ_-, which satisfy the commutation relations $[\sigma_+,\sigma_-]=\sigma_z$ and $[\sigma_z,\sigma_\pm]=\pm 2\sigma_\pm$. In a frame rotating at the frequency ω_L the master equation of the density matrix operator ρ for the combined atom-cavity system is of the form [12,20]

$$\dot{\rho}=-i[H_A+H_C+H_I,\rho]+\mathcal{L}_A\rho+\mathcal{L}_C\rho, \tag{1}$$

where

$$H_A=\frac{\Delta}{2}\sigma_z+\frac{\Omega}{2}(\sigma_++\sigma_-), \tag{2a}$$

$$H_C=\delta a^\dagger a, \tag{2b}$$

$$H_I=g(\sigma_- a^\dagger+\sigma_+ a), \tag{2c}$$

$$\mathcal{L}_A\rho=\gamma(2\sigma_-\rho\sigma_+-\sigma_+\sigma_-\rho-\rho\sigma_+\sigma_-), \tag{2d}$$

$$\mathcal{L}_C\rho=\kappa(2a\rho a^\dagger-a^\dagger a\rho-\rho a^\dagger a), \tag{2e}$$

where H_A and H_C are the unperturbed Hamiltonians for the coherently driven atom and the cavity respectively, while H_I describes the interaction between the atom and the cavity mode. Ω is the Rabi frequency of the driving field, $\Delta=\omega_A-\omega_L$ and $\delta=\omega_C-\omega_L$ are the detunings of the atomic resonance frequency and of the cavity-mode frequency from the driving field frequency, respectively, and g is the coupling constant between the atom and the cavity field. $\mathcal{L}_A\rho$ and $\mathcal{L}_C\rho$, respectively, describe atomic damping to background modes other than the privileged cavity mode, and damping of the cavity field by the standard vacuum reservoir, with γ and κ the atomic and cavity decay constants, respectively. This master equation contains all the essential physics of the system: atom-cavity coupling, driving field, detunings of the atom and of the cavity from the driving field frequency, atomic spontaneous emission, and cavity damping, and has been extensively employed to investigate cavity quantum electrodynamics.

Theoretical studies of the fundamental system are usually performed in the so-called *bad cavity* [11–14] and *good cavity* [17–22] limits, depending upon the parameters g,κ, and γ. The former is ascribed to the regime of weak coupling of the atom to the cavity field with $\kappa\gg g\gg\gamma$, in which the cavity field decay dominates. The cavity field response to the continuum modes is much faster than that produced by its interaction with the atom, so that the atom always experiences the cavity mode in the state induced by the vacuum reservoir. Effectively, the cavity input-output mirror acts as a broadband reservoir of modes, and the atom and cavity maintain essentially individual identities, so that a perturbative description suffices. This is not the situation, however in the strong-coupling regime with $g\gg\kappa,\gamma$, where the internal interaction of the composite atom-cavity system is much larger than that leading to the incoherent decay of the atom and cavity into the external reservoir of modes. In this case, the photon emitted by the atom into the cavity mode is likely to be repeatedly absorbed (since $g\gg\kappa$) and re-emitted (since $g\gg\gamma$) before irreversibly escaping into the environment. Therefore, the system must be described in terms of the structure and dynamics of the composite atom-cavity system (the ''Jaynes-Cummings molecule'') [24].

In this paper we are interested in the bad cavity limit, which is specified by [11,12,14]

$$\kappa\gg g\gg\gamma, \tag{3}$$

but with $C=g^2/\kappa\gamma$ finite, where C is the single-atom cooperativity parameter familiar from optical bistability. In this limit, one can adiabatically eliminate the cavity-mode variables, giving rise to a master equation for the atomic variables only. To do this we at first disregard the atomic spontaneous emission into the background modes, represented by $\mathcal{L}_A\rho$, since this quantity undergoes no change in the elimination procedure.

We first perform a canonical transformation on the master equation (1) by

$$\tilde\rho=e^{i(H_A+H_C)t}\rho e^{-i(H_A+H_C)t}. \tag{4}$$

In the atom-cavity interaction picture the master equation then takes the form

$$\dot{\tilde\rho}=-i[\tilde H_I(t),\tilde\rho]+\mathcal{L}_C\tilde\rho, \tag{5}$$

where

$$\tilde H_I(t)=g[\tilde\sigma_-(t)a^\dagger e^{i\delta t}+\tilde\sigma_+(t)ae^{-i\delta t}], \tag{6a}$$

$$\tilde\sigma_\pm(t)=e^{iH_At}\sigma_\pm e^{-iH_At}. \tag{6b}$$

Equation (5) may be treated by writing it as

$$\partial_t(e^{-\mathcal{L}_Ct}\tilde\rho)=-ie^{-\mathcal{L}_Ct}[\tilde H_I(t),\tilde\rho] \tag{7}$$

and introducing the operator [14,25,26]

$$\chi=e^{-\mathcal{L}_Ct}\tilde\rho. \tag{8}$$

Using Eq. (5) and the relations

$$\begin{aligned}
\mathcal{L}_C(a\tilde\rho)&=a(\mathcal{L}_C\tilde\rho)+\kappa a\tilde\rho,\\
\mathcal{L}_C(\tilde\rho a^\dagger)&=(\mathcal{L}_C\tilde\rho)a^\dagger+\kappa\tilde\rho a^\dagger,\\
\mathcal{L}_C([a,\tilde\rho])&=[a,(\mathcal{L}_C\tilde\rho-\kappa\tilde\rho)],\\
\mathcal{L}_C([a^\dagger,\tilde\rho])&=[a^\dagger,(\mathcal{L}_C\tilde\rho-\kappa\tilde\rho)],
\end{aligned} \tag{9}$$

one obtains [25]

$$\begin{aligned}
\dot\chi(t)=&-ige^{\kappa t}\{[a^\dagger,\tilde\sigma_-(t)\chi(t)]e^{i\delta t}+[a,\chi(t)\tilde\sigma_+(t)]e^{-i\delta t}\}\\
&-ige^{-\kappa t}\{[\tilde\sigma_-(t),\chi(t)a^\dagger]e^{i\delta t}+[\tilde\sigma_+(t),a\chi(t)]e^{-i\delta t}\},
\end{aligned} \tag{10}$$

which involves only the atom-cavity interaction, and resembles the evolution equation of the ideal quantum Jaynes-Cummings model [24] except for the presence of terms in which $\chi(t)$ is sandwiched between operators.

Due to the smallness of the coupling constant g, we can perform a second-order perturbation calculation with respect to g by means of standard projection operator techniques. We now integrate Eq. (10) formally to give

$$\chi(t)=\chi(0)-ig\int_0^t e^{\kappa t'}\{[a^\dagger,\tilde{\sigma}_-(t')\chi(t')]e^{i\delta t'}+[a,\chi(t')\tilde{\sigma}_+(t')]e^{-i\delta t'}\}dt'-ig\int_0^t e^{-\kappa t'}\{[\tilde{\sigma}_-(t'),\chi(t')a^\dagger]e^{i\delta t'}$$
$$+[\tilde{\sigma}_+(t'),a\chi(t')]e^{-i\delta t'}\}dt'. \tag{11}$$

Substituting for $\chi(t)$ inside the commutators in Eq. (10) leads to

$$\dot{\chi}(t)=-ige^{\kappa t}\{[a^\dagger,\tilde{\sigma}_-(t)\chi(0)]e^{i\delta t}+[a,\chi(0)\tilde{\sigma}_+(t)]e^{-i\delta t}\}$$
$$-ige^{-\kappa t}\{[\tilde{\sigma}_-(t),\chi(0)a^\dagger]e^{i\delta t}+[\tilde{\sigma}_+(t),a\chi(0)]e^{-i\delta t}\}$$
$$-g^2e^{(\kappa+i\delta)t}\int_0^t dt'\{[a^\dagger,\tilde{\sigma}_-(t)[a^\dagger,\tilde{\sigma}_-(t')\chi(t')]]e^{(\kappa+i\delta)t'}+[a^\dagger,\tilde{\sigma}_-(t)[a,\chi(t')\tilde{\sigma}_+(t')]]e^{(\kappa-i\delta)t'}$$
$$+[a^\dagger,\tilde{\sigma}_-(t)[\tilde{\sigma}_-(t'),\chi(t')a^\dagger]]e^{-(\kappa-i\delta)t'}+[a^\dagger,\tilde{\sigma}_-(t)[\tilde{\sigma}_+(t'),a\chi(t')]]e^{-(\kappa+i\delta)t'}\}$$
$$-g^2e^{(\kappa-i\delta)t}\int_0^t dt\{[a,[a^\dagger,\tilde{\sigma}_-(t')\chi(t')]\tilde{\sigma}_+(t)]e^{(\kappa+i\delta)t'}+[a,[a,\chi(t')\tilde{\sigma}_+(t')]\tilde{\sigma}_+(t)]e^{(\kappa-i\delta)t'}$$
$$+[a,[\tilde{\sigma}_-(t'),\chi(t')a^\dagger]\tilde{\sigma}_+(t)]e^{-(\kappa-i\delta)t'}+[a,[\tilde{\sigma}_+(t'),a\chi(t')]\tilde{\sigma}_+(t)]e^{-(\kappa+i\delta)t'}\}$$
$$-g^2e^{-(\kappa-i\delta)t}\int_0^t dt'\{[\tilde{\sigma}_-(t),[a^\dagger,\tilde{\sigma}_-(t')\chi(t')]a^\dagger]e^{(\kappa+i\delta)t'}+[\tilde{\sigma}_-(t),[a,\chi(t')\tilde{\sigma}_+(t')]a^\dagger]e^{(\kappa-i\delta)t'}$$
$$+[\tilde{\sigma}_-(t),[\tilde{\sigma}_-(t'),\chi(t')a^\dagger]a^\dagger]e^{-(\kappa-i\delta)t'}+[\tilde{\sigma}_-(t),[\tilde{\sigma}_+(t'),a\chi(t')]a^\dagger]e^{-(\kappa+i\delta)t'}\}$$
$$-g^2e^{-(\kappa+i\delta)t}\int_0^t dt'\{[\tilde{\sigma}_+(t),a[a^\dagger,\tilde{\sigma}_-(t')\chi(t')]]e^{(\kappa+i\delta)t'}+[\tilde{\sigma}_+(t),a[a,\chi(t')\tilde{\sigma}_+(t')]]e^{(\kappa-i\delta)t'}$$
$$+[\tilde{\sigma}_+(t),a[\tilde{\sigma}_-(t'),\chi(t')a^\dagger]]e^{-(\kappa-i\delta)t'}+[\tilde{\sigma}_+(t),a[\tilde{\sigma}_+(t'),a\chi(t')]]e^{-(\kappa+i\delta)t'}\}. \tag{12}$$

We assume that no correlation exists between the atom and the cavity mode at the initial time ($t=0$), that is $\chi(t)=\rho_C(0)\tilde{\rho}_A(0)$. At later times, correlations may arise due to the coupling of the atom to the cavity through H_I. However, we have assumed that the coupling is very weak, and at all times $\chi(t)$ should only show deviations of order H_I from the uncorrelated state. Furthermore, the cavity damping rate κ is much larger than the coupling constant g, and therefore the integrals in Eq. (12) make nonzero contributions only for $t\leqslant\kappa^{-1}$. Over this time scale the cavity should be virtually unaffected by its coupling to the atom. We can thus factorize $\chi(t)$ [14,26].,

$$\chi(t)\simeq\rho_C(0)\tilde{\rho}_A(t), \tag{13}$$

where $\rho_C(0)$ is the density matrix operator of the cavity mode in the absence of the atom and the driving field. Noting that

$$\mathrm{Tr}_C\chi(t)\equiv\mathrm{Tr}_C\tilde{\rho}(t)\equiv\tilde{\rho}_A(t), \tag{14}$$

we obtain the master equation for the reduced density-matrix operator $\tilde{\rho}_A$ of the atom from Eq. (12) by tracing out the cavity variables through the following relations:

$$\mathrm{Tr}_C[aa^\dagger\rho_C(0)]=1,\quad \mathrm{Tr}_C[a^\dagger a\rho_C(0)]=0,$$
$$\mathrm{Tr}_C[a^2\rho_C(0)]=0,\quad \mathrm{Tr}_C[a^{\dagger 2}\rho_C(0)]=0, \tag{15}$$
$$\mathrm{Tr}_C[a\rho_C(0)]=0,\quad \mathrm{Tr}_C[a^\dagger\rho_C(0)]=0.$$

The resulting master equation is then of the form

$$\dot{\tilde{\rho}}_A(t)=-g^2\int_0^t e^{-(\kappa-i\delta)\tau}[\tilde{\rho}_A(t-\tau)\tilde{\sigma}_+(t-\tau)\tilde{\sigma}_-(t)$$
$$-\tilde{\sigma}_-(t)\tilde{\rho}_A(t-\tau)\tilde{\sigma}_+(t-\tau)]d\tau$$
$$-g^2\int_0^t e^{-(\kappa+i\delta)\tau}[\tilde{\sigma}_+(t)\tilde{\sigma}_-(t-\tau)\tilde{\rho}_A(t-\tau)$$
$$-\tilde{\sigma}_-(t-\tau)\tilde{\rho}_A(t-\tau)\tilde{\sigma}_+(t)]d\tau. \tag{16}$$

The assumption that $\kappa\gg g$, in which the interaction of the atom with the cavity mode is negligible during the time $\tau\leqslant\kappa^{-1}$, and the fact that the cavity response time (of order κ^{-1}) tends to zero, validates the Markovian approximation [14,26], i.e.,

$$\tilde{\rho}_A(t-\tau)\simeq\tilde{\rho}_A(t). \tag{17}$$

We can also extend the upper limit of the integrals to infinity. Then transforming $\tilde{\rho}_A$ back to the original picture via $\rho_A = \exp(-iH_A t)\tilde{\rho}_A \exp(iH_A t)$, one obtains the master equation for the atom to be

$$\begin{aligned}\dot{\rho}_A(t) = &-i[H_A, \rho_A(t)] - g^2 \int_0^\infty e^{-(\kappa - i\delta)\tau} [\rho_A(t)\tilde{\sigma}_+(-\tau)\sigma_- \\ &- \sigma_- \rho_A(t)\tilde{\sigma}_+(-\tau)]d\tau \\ &- g^2 \int_0^\infty e^{-(\kappa + i\delta)\tau} [\sigma_+ \tilde{\sigma}_-(-\tau)\rho_A(t) \\ &- \tilde{\sigma}_-(-\tau)\rho_A(t)\sigma_+]d\tau. \end{aligned} \tag{18}$$

In the above equation the first term describes the coherent evolution of the driven atom, whereas the remaining terms represent the cavity-induced atomic decay into the cavity mode. For observation of the cavity-induced fluorescence emission, the cavity must have a window (input-output mirror), so the atom also couples to the modes of the continuum (the background modes). After taking the spontaneous emission to the background modes into account, the complete master equation of the density-matrix operator for the coherently driven atom coupled to the cavity field has the form

$$\begin{aligned}\dot{\rho_A} = &-i[H_A, \rho_A] + \gamma(2\sigma_- \rho_A \sigma_+ - \sigma_+ \sigma_- \rho_A - \rho_A \sigma_+ \sigma_-) \\ &+ \gamma_c(\sigma_- \rho_A S_+ + S_- \rho_A \sigma_+ - \sigma_+ S_- \rho_A - \rho_A S_+ \sigma_-), \end{aligned} \tag{19}$$

where $\gamma_c = \gamma C = g^2/\kappa$ specifies the emission rate of the atom into the cavity mode, and

$$S_- = \kappa \int_0^\infty d\tau\, e^{-(\kappa + i\delta)\tau} \tilde{\sigma}_-(-\tau) = \mathcal{A}_0 \sigma_z + \mathcal{A}_1 \sigma_+ + \mathcal{A}_2 \sigma_-,$$

$$S_+ = (S_-)^\dagger = \mathcal{A}_0^* \sigma_z + \mathcal{A}_1^* \sigma_- + \mathcal{A}_2^* \sigma_+, \tag{20}$$

with

$$\begin{aligned}\mathcal{A}_0 &= \frac{\kappa\Omega}{4\bar{\Omega}^2}\left[\frac{2\Delta}{\kappa + i\delta} - \frac{\bar{\Omega} + \Delta}{\kappa + i(\delta - \bar{\Omega})} + \frac{\bar{\Omega} - \Delta}{\kappa + i(\delta + \bar{\Omega})}\right], \\ \mathcal{A}_1 &= \frac{\kappa\Omega^2}{4\bar{\Omega}^2}\left[\frac{2}{\kappa + i\delta} - \frac{1}{\kappa + i(\delta - \bar{\Omega})} - \frac{1}{\kappa + i(\delta + \bar{\Omega})}\right], \\ \mathcal{A}_2 &= \frac{\kappa}{4\bar{\Omega}^2}\left[\frac{2\Omega^2}{\kappa + i\delta} + \frac{(\bar{\Omega} + \Delta)^2}{\kappa + i(\delta - \bar{\Omega})} + \frac{(\bar{\Omega} - \Delta)^2}{\kappa + i(\delta + \bar{\Omega})}\right], \end{aligned} \tag{21}$$

where $\bar{\Omega} = \sqrt{\Omega^2 + \Delta^2}$ is a generalized Rabi frequency. Obviously, the coefficients $\mathcal{A}_0$, $\mathcal{A}_1$, and $\mathcal{A}_2$ are Rabi frequency dependent, and resonant when the cavity frequency is tuned to $\delta = 0, \pm\bar{\Omega}$, which is reminiscent of the Mollow triplet in free space [1]. The resonance property reflects the fact that when the atom is strongly driven by a laser beam, the atom-laser interaction forms a ''dressed'' atom [3] whose energy-level structure is intensity dependent and whose spontaneous emission dominates at three frequencies: ω_L and $\omega_L \pm \bar{\Omega}$. Therefore, when the cavity is tuned to these three frequencies, atomic transitions are enhanced.

The cavity-modified master equation (19) reduces to Cirac's case [26] when $\delta = 0$. Furthermore, when $\Delta = \delta = 0$ and $\Omega \ll \kappa$, the master equation (19) becomes the one obtained by Rice and Carmichael [11], which is formally similar to that in free space, but with the renormalized decay rate $\gamma(1 + C)$. Otherwise, as we shall see, the atomic radiative properties are significantly modified when the driving field is very strong, and the frequency of the cavity is tuned to either the center or one of the sidebands of the Mollow triplet.

III. BARE-STATE POPULATION INVERSION

From the cavity-modified master equation (19), one can obtain the equations of motion for the reduced density-matrix elements governing the atomic dynamics to be

$$\begin{aligned}\dot{\rho}_{00} &= (2\gamma + \gamma_c \mathcal{A}_2 + \gamma_c \mathcal{A}_2^*)\rho_{11} - \left(\gamma_c \mathcal{A}_0 - i\frac{\Omega}{2}\right)\rho_{01} \\ &\quad - \left(\gamma_c \mathcal{A}_0^* + i\frac{\Omega}{2}\right)\rho_{10}, \\ \dot{\rho}_{11} &= -(2\gamma + \gamma_c \mathcal{A}_2 + \gamma_c \mathcal{A}_2^*)\rho_{11} + \left(\gamma_c \mathcal{A}_0 - i\frac{\Omega}{2}\right)\rho_{01} \\ &\quad + \left(\gamma_c \mathcal{A}_0^* + i\frac{\Omega}{2}\right)\rho_{10}, \\ \dot{\rho}_{01} &= -(\gamma - i\Delta + \gamma_c \mathcal{A}_2^*)\rho_{01} + \gamma_c \mathcal{A}_1^* \rho_{10} + \left(\gamma_c \mathcal{A}_0^* + i\frac{\Omega}{2}\right)\rho_{00} \\ &\quad + \left(\gamma_c \mathcal{A}_0^* - i\frac{\Omega}{2}\right)\rho_{11}, \\ \dot{\rho}_{10} &= -(\gamma + i\Delta + \gamma_c \mathcal{A}_2)\rho_{10} + \gamma_c \mathcal{A}_1 \rho_{01} + \left(\gamma_c \mathcal{A}_0 - i\frac{\Omega}{2}\right)\rho_{00} \\ &\quad + \left(\gamma_c \mathcal{A}_0 + i\frac{\Omega}{2}\right)\rho_{11}, \end{aligned} \tag{22}$$

where ρ_{00} and ρ_{11} are the atomic population in the ground state ($|0\rangle$) and in the excited state ($|1\rangle$), respectively, and ρ_{01} and ρ_{10} describe the atomic ''coherences'' (or ''transitions''). (Here we have dropped the subscript A from the atomic density matrix operator ρ_A for brevity.) One sees from the last two equations of Eqs. (22) that the atomic transition from the ground state to the excited state, ρ_{01}, couples to its conjugate ρ_{10}, a transition from the excited state to the

ground state, due to the cavity effect, which is formally similar to that of a driven two-level atom interacting with a squeezed vacuum reservoir [23].

We may write the equations of motion (22) more simply in a physically transparent, rate-equation form, by eliminating the off-diagonal elements, as

$$\dot{\rho}_{00}=-\mathcal{R}_{01}\rho_{00}+\mathcal{R}_{10}\rho_{11}, \tag{23a}$$

$$\dot{\rho}_{11}=\mathcal{R}_{01}\rho_{00}-\mathcal{R}_{10}\rho_{11}, \tag{23b}$$

where

$$\mathcal{R}_{01}=2\,\mathrm{Re}\left\{\frac{(\gamma+i\Delta+\gamma_c\mathcal{A}_2)\left|\left(\gamma_c\mathcal{A}_0-i\frac{\Omega}{2}\right)\right|^2+\gamma_c\mathcal{A}_1^*\left(\gamma_c\mathcal{A}_0-i\frac{\Omega}{2}\right)^2}{|(\gamma+i\Delta+\gamma_c\mathcal{A}_2)|^2-|\gamma_c\mathcal{A}_1|^2}\right\},$$

$$\mathcal{R}_{10}=2\gamma+2\gamma_c\mathrm{Re}(\mathcal{A}_2)-2\,\mathrm{Re}\left\{\frac{\left(\gamma_c\mathcal{A}_0-i\frac{\Omega}{2}\right)\left[(\gamma+i\Delta+\gamma_c\mathcal{A}_2)\left(\gamma_c\mathcal{A}_0^*-i\frac{\Omega}{2}\right)+\gamma_c\mathcal{A}_1^*\left(\gamma_c\mathcal{A}_0+i\frac{\Omega}{2}\right)\right]}{|(\gamma+i\Delta+\gamma_c\mathcal{A}_2)|^2-|\gamma_c\mathcal{A}_1|^2}\right\}, \tag{24}$$

respectively, are the transition rate from the ground state $|0\rangle$ to the excited state $|1\rangle$ and from the excited state to the ground state. Thus Eq. (23a) expresses the fact that the rate of change of the population in the ground state $|0\rangle$ is equal to the difference between the rate of transitions *out of* state $|0\rangle$ (the first term on the right-hand side) and the rate of transitions *into* $|0\rangle$ (the second term). The rate equations (23a) and (23b) accurately describe the long-time behavior of the coherently driven atom coupled to the single-mode cavity field in the bad cavity limit, and will give the exact solution for the steady state.

The steady-state populations are given, respectively, by

$$\rho_{00}=\frac{\mathcal{R}_{10}}{\mathcal{R}_{01}+\mathcal{R}_{10}}, \quad \rho_{11}=\frac{\mathcal{R}_{01}}{\mathcal{R}_{01}+\mathcal{R}_{10}}. \tag{25}$$

In free space, $\mathcal{R}_{01}$ and $\mathcal{R}_{10}$ read, respectively,

$$\mathcal{R}_{01}=\frac{\gamma\Omega^2}{2(\gamma^2+\Delta^2)}, \quad \mathcal{R}_{10}=2\gamma+\frac{\gamma\Omega^2}{2(\gamma^2+\Delta^2)}, \tag{26}$$

where $\mathcal{R}_{01}$ may be interpreted as the absorption rate excited by the coherent driving field, while $\mathcal{R}_{10}$ is composed of an incoherent spontaneous emission rate, represented by 2γ, and a stimulated emission rate, represented by the remaining term, which is the same as the absorption rate. The coherent driving field thus tends to equalize the population distribution, while the incoherent spontaneous decay tends to bring the population down irreversibly. $\mathcal{R}_{01}$ is always less than $\mathcal{R}_{10}$, and it is therefore impossible to achieve population inversion for the driven two-level atom in free space; that is $\rho_{11}<\rho_{00}$ always holds.

However, the presence of a cavity will modify the conclusion markedly. For example, in the case in which both the atom and cavity are in resonance with the driving laser, i.e., $\Delta=0$, and $\delta=0$, the rates of transitions $\mathcal{R}_{01}$ and $\mathcal{R}_{01}$ reduce to

$$\mathcal{R}_{01}=\frac{\Omega^2}{2(\gamma+\gamma_c)}\left(1+\frac{\gamma_c\kappa}{\kappa^2+\Omega^2}\right)^2, \tag{27}$$

$$\mathcal{R}_{10}=2\gamma+\gamma_c+\gamma_c\frac{\kappa^2}{\kappa^2+\Omega^2}+\frac{\Omega^2}{2(\gamma+\gamma_c)}\left[1-\left(\frac{\gamma_c\kappa}{\kappa^2+\Omega^2}\right)^2\right].$$

In this case, the stimulated emission rate is not equal to the absorption rate. These expressions allow one to gain physical insight into how the atom-cavity coupling and the coherent driving field can modify the atomic radiative properties. We assume, for simplicity, that the Rabi frequency Ω is much less than the cavity decay rate κ. One then has the transition rates

$$\mathcal{R}_{01}\simeq\frac{\Omega^2}{2\gamma_T}+\left(\frac{g}{\kappa}\right)^2\left[2+\left(\frac{g}{\kappa}\right)^2\right]\frac{\Omega^2}{2\gamma_T}, \tag{28a}$$

$$\mathcal{R}_{10}\simeq 2\gamma_T+\frac{\Omega^2}{2\gamma_T}-\left(\frac{g}{\kappa}\right)^4\frac{\Omega^2}{2\gamma_T}, \tag{28b}$$

where $\gamma_T=\gamma+\gamma_c$ is the total emission rate of the atom into the background modes and the cavity mode. The first term on the right-hand side of Eq. (28a) is formally the same as the absorption rate excited by the coherent laser in free space, whereas the second term is a cavity-induced absorption rate which is proportional to $(g/\kappa)^2$ as well as to Ω^2. For Eq. (28b), the first and second terms represent the incoherent and coherent spontaneous emission respectively, as in free space. The last term, however, which is induced by the cavity, tends to decrease the stimulated emission rate. Hence increasing the atom-cavity coupling strength g and Rabi frequency Ω may enhance the absorption rate while inhibiting the total emission rate. If g and Ω are large enough, one may have $\mathcal{R}_{01}>\mathcal{R}_{10}$, so that population inversion takes place.

After straightforward algebra, one finds from Eq. (27) that $\mathcal{R}_{01}>\mathcal{R}_{10}$ when the Rabi frequency obeys

$$\Omega>\left[\frac{2(\gamma+\gamma_c+\kappa)(\gamma+\gamma_c)^2\kappa^2}{(\gamma+2\gamma_c+\kappa)[\gamma_c\kappa-(\gamma+\gamma_c)(2\gamma+\gamma_c)]}\right]^{1/2}, \tag{29}$$

and population inversion ($\rho_{11}>\rho_{00}$) is achieved.

We now present the numerical results of the cavity-induced population inversion for high driving intensities.

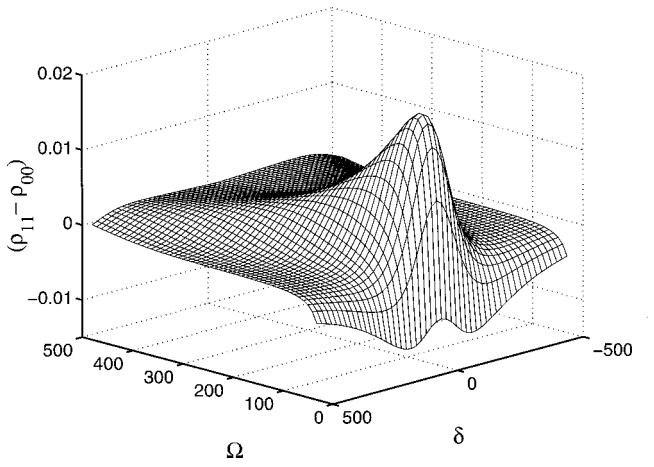

FIG. 1. The population difference $(\rho_{11}-\rho_{00})$ between the excited state $|1\rangle$ and the ground state $|0\rangle$, as a function of the cavity detuning δ and Rabi frequency Ω, for $\gamma=1$, $g=20$, $\kappa=100$, and $\Delta=0$.

Throughout these graphs we set $\gamma=1,\kappa=100$, and $g=10-30$ (bad cavity) in order to study the role of the atom-cavity coupling in the population dynamics.

Figure 1 displays the population difference $(\rho_{11}-\rho_{00})$ as a function of the Rabi frequency Ω and the cavity detuning δ, for the parameters $\gamma=1$, $g=20$, $\kappa=100$, and $\Delta=0$. One sees that for small Rabi frequencies $\Omega\ll\kappa$ the population of the ground state is greater than that of the excited state for all values of δ. However, the atomic population may be inverted for larger Rabi frequencies. For intermediate values $(\Omega\sim\kappa)$, the population inversion is maximal at $\delta=0$, and this is a global maximum, yielding an inversion of almost 2%. As Ω increases beyond the value $\Omega=\kappa$, the maximum at $\delta=0$ decreases and eventually turns into a minimum. For large Rabi frequencies $(\Omega\gg\kappa)$, the population inversion is resonant when $\delta\sim\pm\Omega$. These unusual features are more clearly shown in Fig. 2. From Fig. 2(a), where $\delta=0$, one finds that when $\Omega>36$, the value of Eq. (29), the population is inverted $(\rho_{11}-\rho_{00}>0)$. The population inversion reaches a maximum value (0.0181) at the Rabi frequency $\Omega\sim72$, and then decreases as Ω increases. In Fig. 2(b), we set $\Omega=500\gg\kappa$, and the population inversion occurs over the range $-500<\delta<500$. The maximum of the inversion occurs at $|\delta|\sim330$, while there is a minimum in the inversion at $\delta=0$.

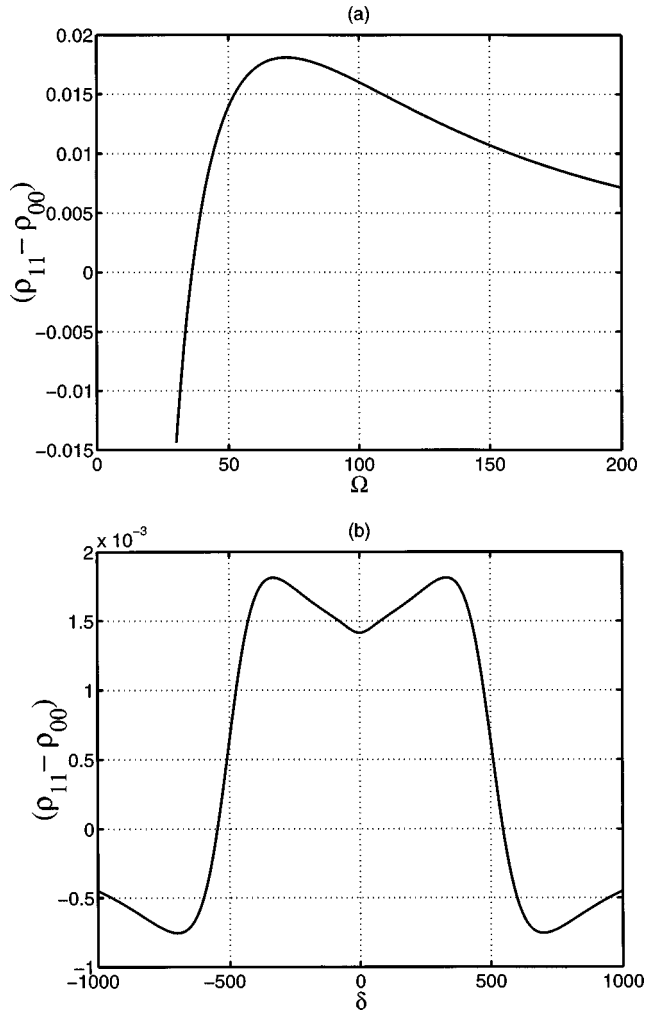

FIG. 2. Same as Fig. 1, but two-dimensional plots for clarity. In frame (a), $\delta=0$, and in frame (b), $\Omega=500$.

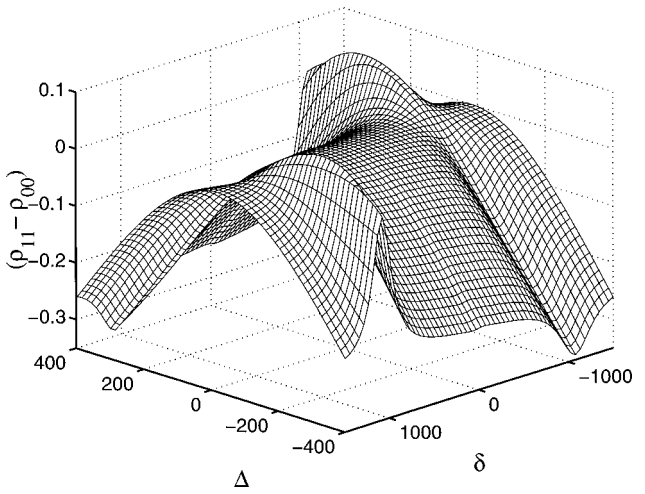

FIG. 3. Same as Fig. 1, but against the detunings δ and Δ, for $\gamma=1$, $g=20$, $\kappa=100$, and $\Omega=1000$.

We display the population difference against the detunings Δ and δ, for $\gamma=1$, $g=20$, $\kappa=100$, and $\Omega=1000$, in Fig. 3, from which one can see that the difference is resonant at $\delta=\pm\bar{\Omega}$. For the atomic detuning $\Delta>0$, when the cavity frequency is tuned to $\delta=\bar{\Omega}$, the population difference $(\rho_{11}-\rho_{00})$ is negative, while it is positive (population inversion) when the cavity is tuned to $\delta=-\bar{\Omega}$. For $\Delta<0$ the situation is reversed. It is clear that quite large inversions (>0.05) arise for $\delta\simeq\bar{\Omega}$ and $\Delta\simeq300$. The resonance profiles of the population difference are similar to those of the atomic fluorescence observed in Ref. [15]. This reflects the fact that the intensity of the atomic fluorescence light is proportional to the population of the excited state, that is,

$$I=\rho_{11}=\frac{1}{2}+\frac{\rho_{11}-\rho_{00}}{2}. \tag{30}$$

Hence the fluorescence emission can be enhanced or suppressed when the cavity is tuned to $\delta=\pm\bar{\Omega}$. The enhance-

ment of the atomic fluorescence is a direct consequence of the atomic population inversion.

In Fig. 4, we show the effect of various atom-cavity coupling constants g on the population inversion, for $\gamma=1$, $\kappa=100$, and $\Omega=500$, with $\Delta=0$ in Fig. 4(a) and $\Delta=100$ in Fig. 4(b). Both cases clearly exhibit that the stronger the coupling, the greater the population inversion. This therefore implies that the population may be highly inverted in the strong-coupling regime [20]. (Note that as our formulas are based on the bad cavity assumption, $\kappa \gg g \gg \gamma$, we cannot make g arbitrarily large.)

IV. DRESSED-STATE POPULATION INVERSION

The resonance properties with the cavity frequency tuned to the center and sidebands of the Mollow triplet can be understood in the semiclassical dressed-state $|\pm\rangle$ representation. The dressed states, defined by the eigenvalue equation $H_A|\pm\rangle=\pm(\bar{\Omega}/2)|\pm\rangle$, are associated with the bare atomic states $|0\rangle$, and $|1\rangle$ through

$$\begin{aligned} |+\rangle &= s|0\rangle + c|1\rangle, \\ |-\rangle &= c|0\rangle - s|1\rangle, \end{aligned} \tag{31}$$

where

$$c=\sqrt{\frac{\bar{\Omega}+\Delta}{2\bar{\Omega}}}, \quad s=\sqrt{\frac{\bar{\Omega}-\Delta}{2\bar{\Omega}}}. \tag{32}$$

The rate equations in the dressed-state representation are given by

$$\begin{aligned} \dot{\rho}_{--} &= -\mathcal{R}_{-+}\rho_{--} + \mathcal{R}_{+-}\rho_{++}, \\ \dot{\rho}_{++} &= \mathcal{R}_{-+}\rho_{--} - \mathcal{R}_{+-}\rho_{++}, \end{aligned} \tag{33}$$

where ρ_{++}, and ρ_{--} are the populations of the dressed states $|+\rangle$ and $|-\rangle$ respectively, and $\mathcal{R}_{+-}$ is the atomic transition rate from the substate $|+\rangle$ of one dressed-state doublet to the substate $|-\rangle$ of the dressed-state doublet below, whereas $\mathcal{R}_{-+}$ describes the transition rate from the state $|-\rangle$ of one dressed-state doublet to the state $|+\rangle$ of the next dressed-state doublet, as depicted in Fig. 5. The stationary dressed state populations can be expressed as

$$\rho_{--}=\frac{\mathcal{R}_{+-}}{\mathcal{R}_{+-}+\mathcal{R}_{-+}}, \quad \rho_{++}=\frac{\mathcal{R}_{-+}}{\mathcal{R}_{+-}+\mathcal{R}_{-+}}. \tag{34}$$

Both $\mathcal{R}_{-+}$ and $\mathcal{R}_{+-}$ are in general very complicated. However, if the Rabi frequency is very large, $\bar{\Omega} \gg \kappa, g, \gamma$, then $\mathcal{R}_{-+}$ and $\mathcal{R}_{+-}$ can be enormously simplified by invoking the secular approximation [3], with the physics remaining clear. They then have the forms

$$\begin{aligned} \mathcal{R}_{-+} &= 2\gamma s^4 + 2\gamma_c s^4 \frac{\kappa^2}{\kappa^2+(\delta+\bar{\Omega})^2}, \\ \mathcal{R}_{+-} &= 2\gamma c^4 + 2\gamma_c c^4 \frac{\kappa^2}{\kappa^2+(\delta-\bar{\Omega})^2}. \end{aligned} \tag{35}$$

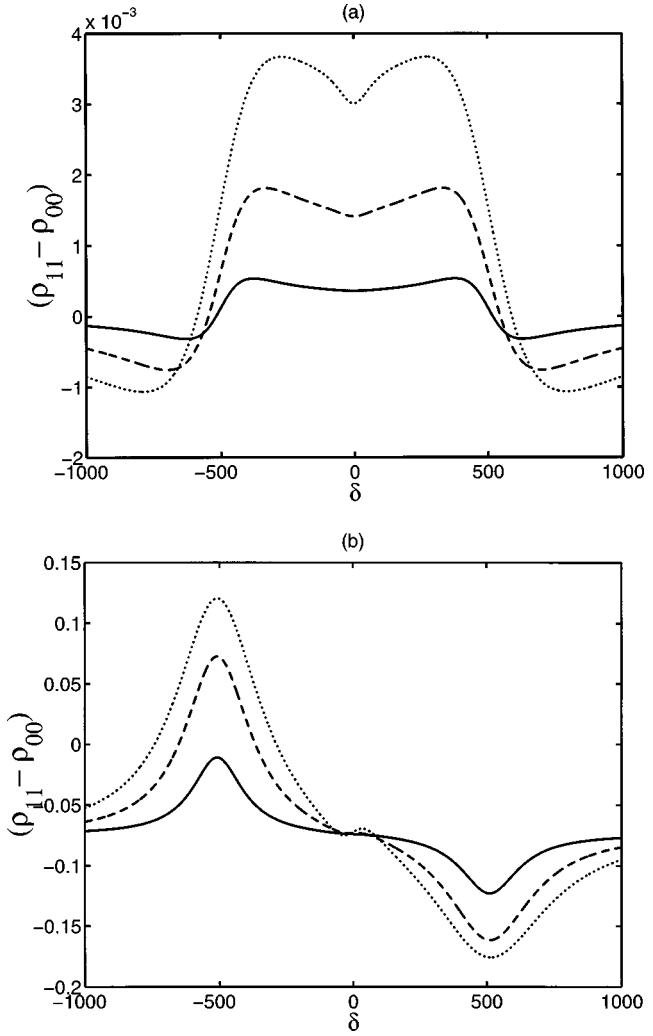

FIG. 4. Two-dimensional plots of the population difference against δ, for $\gamma=1$, $\kappa=100$, and $\Omega=500$, and different atom-cavity couplings: $g=10$ (solid line), $g=20$ (dashed line), and $g=30$ (dotted line). In frame (a), $\Delta=0$, and in frame (b), $\Delta=100$.

It is well known that in free space both $\mathcal{R}_{-+}$ and $\mathcal{R}_{+-}$, represented by the first term on the right-hand side of Eq. (35), are the same when the atom is in resonance with the driving field, i.e., $\Delta=0$, so that the atomic population is evenly distributed between the dressed states $|\pm\rangle$.

However, in the presence of the cavity, the transition rates $\mathcal{R}_{-+}$ and $\mathcal{R}_{+-}$ are strongly dependent on the cavity frequency, as displayed in Eq. (35). For example, if the atomic frequency is resonant with the laser frequency ($\Delta=0$), and the cavity is tuned to resonance with the driving field ($\delta=0$), then $\mathcal{R}_{-+}=\mathcal{R}_{+-}$, and there is thus no population difference between the dressed states. However, if the cavity frequency is tuned to the left sideband of the Mollow triplet, that is $\delta=-\bar{\Omega}$, the transition rates reduce to

$$\mathcal{R}_{-+}=\frac{\gamma+\gamma_c}{2}, \quad \mathcal{R}_{+-}\simeq\frac{\gamma}{2}. \tag{36}$$

The symmetry of transitions between the dressed states is broken. The populations then have the form

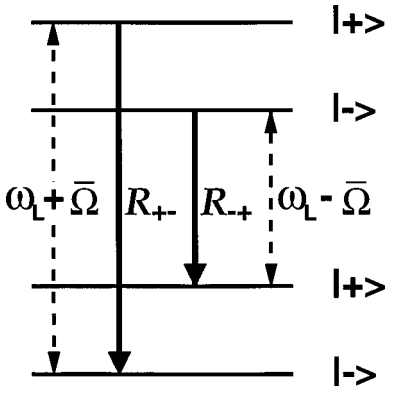

FIG. 5. Diagram of atomic dressed states and dressed-state transitions.

$$\rho_{--} \simeq \frac{\gamma}{2\gamma+\gamma_c} = \frac{1}{2+C}, \qquad \rho_{++} \simeq \frac{\gamma+\gamma_c}{2\gamma+\gamma_c} = \frac{1+C}{2+C}. \tag{37}$$

It is obvious that $\rho_{++} > \rho_{--}$: dressed-state population inversion is achieved. If $C \gg 2$, the atomic population can be approximately trapped in the dressed state $|+\rangle$.

For $\delta = \bar{\Omega}$—that is, the cavity is in resonance with the right sideband of the Mollow triplet—the transition rates and the populations, respectively, are given by

$$\mathcal{R}_{-+} \simeq \frac{\gamma}{2}, \quad \mathcal{R}_{+-} = \frac{\gamma+\gamma_c}{2}, \tag{38}$$

$$\rho_{--} \simeq \frac{\gamma+\gamma_c}{2\gamma+\gamma_c} = \frac{1+C}{2+C}, \quad \rho_{++} \simeq \frac{\gamma}{2\gamma+\gamma_c} = \frac{1}{2+C}, \tag{39}$$

where $\mathcal{R}_{-+} < \mathcal{R}_{+-}$ and the population is hence gathered in the dressed state $|-\rangle$ when $C \gg 2$.

The unbalanced population distribution between the dressed states $|\pm\rangle$ results from the cavity-induced enhancement or inhibition of the population transition rates. One can see in Fig. 5 that the atomic transition from the dressed state $|+\rangle$ to the dressed state $|-\rangle$, at the rate $\mathcal{R}_{+-}$, occurs at frequency $\omega_L + \bar{\Omega}$, while the transition from $|-\rangle$ to $|+\rangle$, at rate $\mathcal{R}_{-+}$, takes place at frequency $\omega_L - \bar{\Omega}$. If the driven atom is inside a cavity, whose frequency is tuned to the right-hand sideband of the Mollow spectrum, $\delta = \omega_C - \omega_L = \bar{\Omega}$, the atomic transition $\mathcal{R}_{+-}$ is thus resonant with the cavity. The interaction of the atom with the privileged cavity mode is enhanced, and the atom predominantly (since $g \gg \gamma$) emits a photon into the cavity mode, described by $\gamma_c/2$, besides emitting a photon into the background modes, presented by $\gamma/2$. However, the transition $\mathcal{R}_{-+}$, at the frequency $\omega_L - \bar{\Omega}$, is far off resonance with the cavity (since $\bar{\Omega} \gg \kappa$), so the atom can only emit a photon into the background modes. The atomic transition at the frequency $\omega_L + \bar{\Omega}$ is enhanced by the atom-cavity coupling. As a consequence, there are more populations in the dressed state $|-\rangle$. Similarly, if the cavity is resonant with the left-hand sideband, $\delta = -\bar{\Omega}$, the atomic transition rate $\mathcal{R}_{-+}$ at the cavity frequency $\omega_L - \bar{\Omega}$ is resonantly enhanced. The population is most likely to be in the dressed state $|+\rangle$.

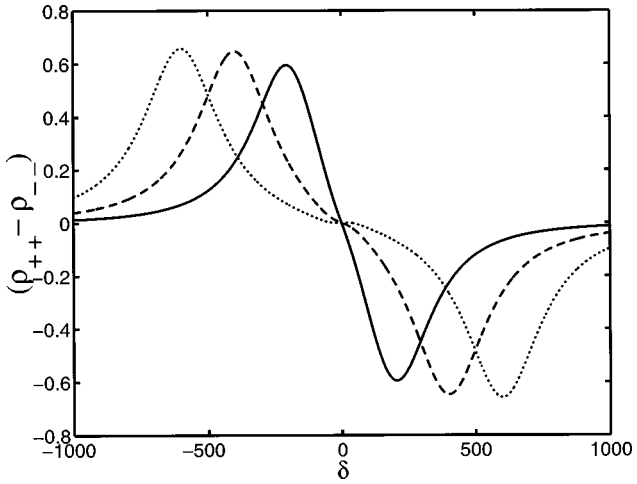

FIG. 6. Two-dimensional plots of the population difference $(\rho_{++} - \rho_{--})$ between the dressed states $|+\rangle$ and $|-\rangle$, against δ, for $\gamma = 1$, $g = 20$, $\kappa = 100$, and different Rabi frequencies: $\Omega = 200$ (solid line), $\Omega = 400$ (dashed line), and $\Omega = 600$ (dotted line).

We present the exact (without secular approximation) steady-state population difference between the dressed states $|+\rangle$ and $|-\rangle$ in Figs. 6 and 7. From both graphs one can see that the dressed-state population difference is resonant with the cavity frequency tuned to $\delta = \pm\bar{\Omega}$. One can have either $\rho_{++} > \rho_{--}$ (dressed-state population inversion) or $\rho_{--} > \rho_{++}$ (opposite dressed-state population inversion), depending on the cavity resonant frequency. A high population inversion may be achieved by increasing the atom-cavity coupling constant. One can also see that the populations are the same when both the cavity and the atom are in resonance with the laser frequency.

We shall see in Secs. VI and VII that the uneven dressed-state population distribution will give rise to an asymmetry

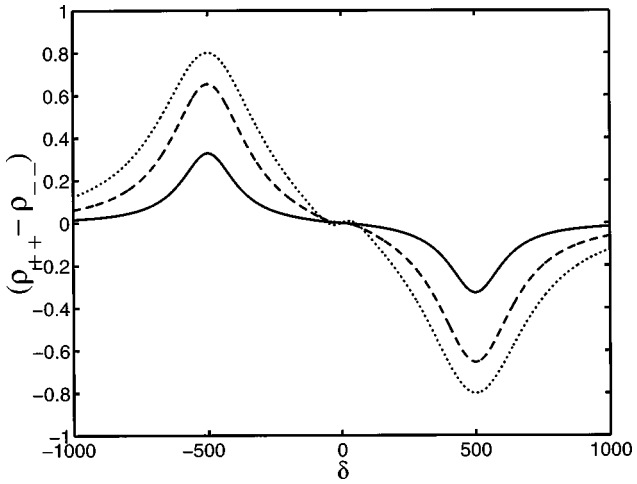

FIG. 7. Same as Fig. 6, but for $\gamma = 1$, $\kappa = 100$, $\Omega = 500$, and different atom-cavity couplings: $g = 10$ (solid line), $g = 20$ (dashed line), and $g = 30$ (dotted line).

in the Mollow fluorescence triplet and a sideband gain in the probe absorption spectrum. The former was observed by Lezama *et al.* [16] in strongly driven two-level atoms coupled to a frequency-dependent vacuum reservoir (a kind of cavity).

V. CAVITY-MODIFIED RELAXATION RATES

For convenience, we rewrite the cavity-modified equations of motion (22), in terms of the in-phase and out-of-phase quadrature amplitudes of the atomic polarization, $\langle\sigma_x\rangle=\langle\sigma_-\rangle+\langle\sigma_+\rangle$ and $\langle\sigma_y\rangle=i(\langle\sigma_-\rangle-\langle\sigma_+\rangle)$, and the atomic population difference $\langle\sigma_z\rangle$:

$$\begin{aligned}\langle\dot\sigma_x\rangle&=-\gamma_x\langle\sigma_x\rangle-\Delta_y\langle\sigma_y\rangle+\Omega_x,\\ \langle\dot\sigma_y\rangle&=-\gamma_y\langle\sigma_y\rangle+\Delta_x\langle\sigma_x\rangle-\Omega\langle\sigma_z\rangle-\Omega_y,\\ \langle\dot\sigma_z\rangle&=-\gamma_z\langle\sigma_z\rangle+\Omega_x\langle\sigma_x\rangle+(\Omega-\Omega_y)\langle\sigma_y\rangle-\gamma_z,\end{aligned}\tag{40}$$

where

$$\begin{aligned}\Omega_x&=2\gamma_c\mathrm{Re}(\mathcal{A}_0),\\ \Omega_y&=2\gamma_c\mathrm{Im}(\mathcal{A}_0),\\ \Delta_x&=\Delta+\gamma_c\mathrm{Im}(\mathcal{A}_2-\mathcal{A}_1),\\ \Delta_y&=\Delta+\gamma_c\mathrm{Im}(\mathcal{A}_2+\mathcal{A}_1).\end{aligned}\tag{41}$$

The relaxation rates of the in-phase and out-of-phase quadrature amplitudes of the polarization, and the population difference are given, respectively, by

$$\begin{aligned}\gamma_x&=\gamma+\gamma_c\mathrm{Re}(\mathcal{A}_2-\mathcal{A}_1)=\gamma+\frac{\gamma_c\kappa^2}{2\bar\Omega}\left[\frac{\bar\Omega+\Delta}{\kappa^2+(\delta-\bar\Omega)^2}\right.\\ &\left.+\frac{\bar\Omega-\Delta}{\kappa^2+(\delta+\bar\Omega)^2}\right],\\ \gamma_y&=\gamma+\gamma_c\mathrm{Re}(\mathcal{A}_2+\mathcal{A}_1)=\gamma+\frac{\gamma_c\kappa^2}{2\bar\Omega^2}\left[\frac{2\Omega^2}{\kappa^2+\delta^2}\right.\\ &\left.+\frac{\Delta(\bar\Omega+\Delta)}{\kappa^2+(\delta-\bar\Omega)^2}-\frac{\Delta(\bar\Omega-\Delta)}{\kappa^2+(\delta+\bar\Omega)^2}\right],\\ \gamma_z&=\gamma_x+\gamma_y=2\gamma+\frac{\gamma_c\kappa^2}{2\bar\Omega^2}\left[\frac{2\Omega^2}{\kappa^2+\delta^2}+\frac{(\bar\Omega+\Delta)^2}{\kappa^2+(\delta-\bar\Omega)^2}\right.\\ &\left.+\frac{(\bar\Omega-\Delta)^2}{\kappa^2+(\delta+\bar\Omega)^2}\right].\end{aligned}\tag{42}$$

For the specified cavity decay and atom-cavity coupling constant, these relaxation rates depend on the Rabi frequency of the driving field and resonate when the cavity frequency is tuned to the center and to the sidebands of the Mollow fluorescence spectrum. All the resonant linewidths are the same, 2κ.

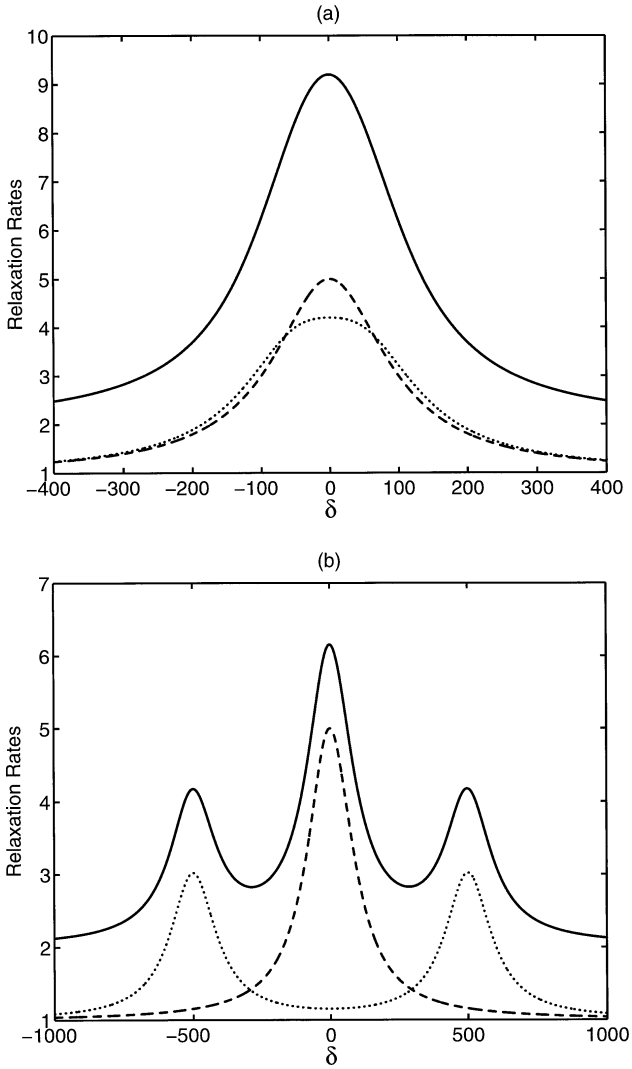

FIG. 8. The cavity-modified relaxation rates γ_x, γ_y, and γ_z of the phase quadratures of the atomic polarization and the atomic population, against the cavity-laser detuning $\delta=\omega_C-\omega_L$, for the parameters $\gamma=1$, $g=20$, $\kappa=100$, $\Delta=0$, and $\Omega=50$ in frame (a), and $\Omega=500$ in frame (b). γ_x, γ_y, and γ_z are represented by dotted, dashed, and solid lines, respectively.

Figure 8, where $\gamma=1$, $g=20$, $\kappa=100$, and $\Delta=0$, displays the cavity-modified relaxation rates of the atomic polarization quadratures and population for $\Omega=50$ in frame (a), and $\Omega=500$ in frame (b), as a function of the cavity frequency δ (taking ω_L fixed). One finds that for a Rabi frequency small compared to the cavity decay rate κ, all the relaxation rates γ_x, γ_y, and γ_z are resonant with the cavity frequency tuned to the atomic transition frequency (or equivalently, the driving-field frequency, as $\Delta=0$). However, when $\Omega\gg\kappa$, γ_x splits into two peaks located at the Mollow sidebands, while γ_y is resonant at the atomic transition frequency, and γ_z has peaks at all three frequencies of the Mollow triplet. Figure 8(b) also shows that for large Rabi frequency γ_y dominates γ_x around $\delta=0$, whereas γ_x dominates γ_y at $\delta\simeq\pm\Omega$. This reflects the dynamical suppression of the cavity-induced relaxation rates of the polarization quadra-

tures of the atom. For example, when the atom is resonant with the driving laser field (i.e., $\Delta=0$), then for the cavity frequency tuned to the center of the Mollow fluorescence triplet, $\delta=0$, one has

$$\gamma_x=\gamma+\gamma_c\frac{\kappa^2}{\kappa^2+\Omega^2},\quad \gamma_y=\gamma+\gamma_c. \tag{43}$$

Therefore in the limit $\Omega\gg\kappa$, the cavity-induced decay rate, associated with γ_c, of the in-phase quadrature is completely suppressed, that is $\gamma_x\simeq\gamma$, while γ_y is independent of the Rabi frequency. However, for $\delta=\Omega$, γ_x and γ_y reduce to

$$\gamma_x=\gamma+\frac{\gamma_c}{2}+\frac{\gamma_c}{2}\frac{\kappa^2}{\kappa^2+4\Omega^2},\quad \gamma_y=\gamma+\gamma_c\frac{\kappa^2}{\kappa^2+\Omega^2}. \tag{44}$$

In the limit $\Omega\gg\kappa$, the cavity-induced decay rate of the out-of-phase quadrature is completely suppressed, whereas the rate of the in-phase quadrature is reduced to $\gamma+\gamma_c/2$. The suppression of the cavity-induced decay rates of the phase quadratures of the atomic polarization will give rise to spectral narrowing of the resonance fluorescence and probe absorption.

VI. RESONANCE FLUORESCENCE SPECTRUM

The incoherent fluorescence spectrum of the atom, emitted from the side of the cavity, can be expressed in terms of the two-time correlation of the atomic operators as [11,17,22]

$$\Lambda(\omega)=\mathrm{Re}\int\lim_{t\to\infty}\langle\sigma_+(t+\tau),\sigma_-(t)\rangle\exp(-i\omega\tau)d\tau, \tag{45}$$

$$\Lambda(\omega)=\frac{1}{2}\mathrm{Re}\left\{\frac{[(z+\gamma_z)(z+\gamma_y+i\Delta_x)+\Omega(\Omega-\Omega_y-i\Omega_x)]\alpha_1-[\Delta_y-i(z+\gamma_x)][(z+\gamma_z)\alpha_2-\Omega\alpha_3]}{(z+\gamma_x)[(z+\gamma_y)(z+\gamma_z)+\Omega(\Omega-\Omega_y)]+\Delta_y[\Delta_x(z+\gamma_z)-\Omega\Omega_x]}\right\}_{z=i\omega}, \tag{46}$$

with

$$\alpha_1=\frac{1}{2}(1+\langle\sigma_z\rangle_s-\langle\sigma_x\rangle_s^2+i\langle\sigma_x\rangle_s\langle\sigma_y\rangle_s),$$

$$\alpha_2=-\frac{i}{2}(1+\langle\sigma_z\rangle_s-\langle\sigma_y\rangle_s^2-i\langle\sigma_x\rangle_s\langle\sigma_y\rangle_s), \tag{47}$$

$$\alpha_3=-\frac{1}{2}(1+\langle\sigma_z\rangle_s)(\langle\sigma_x\rangle_s-i\langle\sigma_y\rangle_s),$$

where

$$\langle\sigma_x\rangle_s=\frac{\Omega_x\gamma_y\gamma_z+(\Omega-\Omega_y)(\Omega\Omega_x-\Delta_y\gamma_z)}{\gamma_z(\gamma_x\gamma_y+\Delta_x\Delta_y)-\Omega\Omega_x\Delta_y+\Omega\gamma_x(\Omega-\Omega_y)},$$

$$\langle\sigma_y\rangle_s=\frac{\gamma_x\gamma_z(\Omega-\Omega_y)-\Omega_x(\Omega\Omega_x-\Delta_x\gamma_z)}{\gamma_z(\gamma_x\gamma_y+\Delta_x\Delta_y)-\Omega\Omega_x\Delta_y+\Omega\gamma_x(\Omega-\Omega_y)}, \tag{48}$$

$$\langle\sigma_z\rangle_s=\frac{-\gamma_z(\gamma_x\gamma_y+\Delta_x\Delta_y)+\Omega_x(\gamma_y\Omega_x+\Delta_y\Omega_y)+(\Omega-\Omega_y)(\Delta_x\Omega_x-\gamma_x\Omega_y)}{\gamma_z(\gamma_x\gamma_y+\Delta_x\Delta_y)-\Omega\Omega_x\Delta_y+\Omega\gamma_x(\Omega-\Omega_y)}$$

are the steady-state solutions of the in-phase and out-of phase quadratures of the atomic polarization and the population difference.

We can gain a general insight into the spectral structures through a study of the poles of $\Lambda(\omega)$, whose real parts determine the widths, and the imaginary parts the positions, of the fluorescence lines. For example, in the case of $\Delta=\delta=0$, the poles of $\Lambda(\omega)$ are at

$$z_0=-\gamma_x,\quad z_\pm=-\frac{\gamma_y+\gamma_z}{2}\pm\sqrt{\left(\frac{\gamma_z-\gamma_y}{2}\right)^2-\Omega(\Omega-\Omega_y)}. \tag{49}$$

The spectrum, in general, consists of three components. The first one is located at line center with linewidth $2\gamma_x$, which arises from the free decay, at the rate γ_x, of the in-phase quadrature amplitude of the atomic polarization. [For $\Delta=\delta$

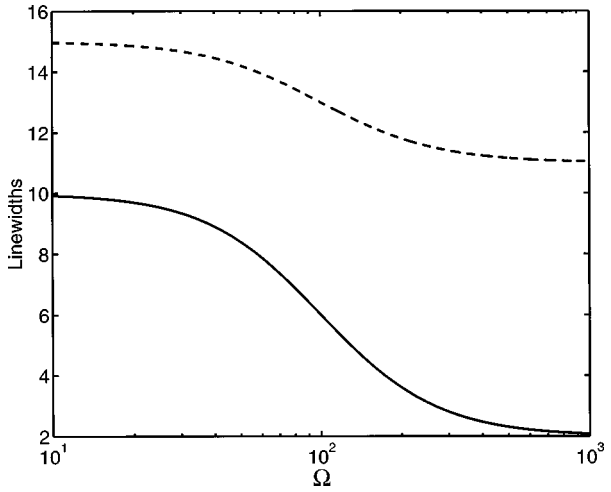

FIG. 9. The linewidths of the central peak (solid line) and the sideband (dashed line) of the incoherent resonance fluorescence spectrum for $\gamma=1$, $g=20$, $\kappa=100$, $\Delta=0$, and $\delta=0$, against the Rabi frequency Ω.

$=0$, $\langle\sigma_x\rangle$ is decoupled from the other Pauli matrices in Eq. (40).] However, the remaining components result from the evolution of the coupled out-of-phase quadrature amplitude of the atomic polarization $\langle\sigma_y\rangle$ and the atomic population inversion $\langle\sigma_z\rangle$. Their positions are dependent on the Rabi frequency Ω. For instance, when the Rabi frequency Ω is less than approximately $(\gamma+\gamma_c)/2$, the poles $z_\pm$ are real, so both components contribute a single peak located at line center with linewidths of approximately $2\gamma_y$ and $2\gamma_z$. As Ω increases, the poles $z_\pm$ become imaginary. Both components then split into two sidebands, but with the same width $(\gamma_y+\gamma_z)$. At large values of Ω, the sidebands are well resolved and placed at $\pm(\Omega-\Omega_y/2)$. These results are similar to the Mollow spectrum in free space [1].

The departures from the free-space situation are that the linewidths of the Mollow-like triplet in the cavity are Rabi frequency dependent, and that the sidebands are shifted by $-\Omega_y/2$. The former can be found from Eq. (43). For a small Rabi frequency, the central linewidth $2\gamma_x\simeq 2(\gamma+\gamma_c)$, and the sideband linewidth $\gamma_y+\gamma_z\simeq 3(\gamma+\gamma_c)$. In the limit of $\Omega\gg\kappa$, however, the width of the central peak reduces to 2γ, whereas the sideband linewidth is $3\gamma+2\gamma_c$. In Fig. 9, we demonstrate the numerical results for the linewidths of the central peak and the sideband of the fluorescence spectrum for $\gamma=1$, $g=20$, $\kappa=100$, $\Delta=0$, and $\delta=0$, against the Rabi frequency Ω. It is clear that the larger the Rabi frequency, the narrower the spectral lines. The narrowing of the spectrum is due to the dynamical suppression of atomic spontaneous emission into the cavity mode [13].

Figure 10 presents the full spectra of the atomic fluorescence emitted out the side of the cavity for the parameters $\gamma=1$, $g=30$, $\kappa=100$, $\Delta=0$, and $\Omega=100$ in frames (a)–(c) and $\Omega=500$ in frames (d)–(f). The cavity frequency is tuned, respectively, to the lower-frequency sideband of the Mollow triplet ($\delta=-\Omega$) in (a) and (d), to the center ($\delta=0$) in (b) and (e), and to the higher-frequency sideband ($\delta=\Omega$) in (c) and (f). One observes that the resonance fluorescence spectra are asymmetric when the cavity frequency is tuned to the Mollow sidebands. Moreover, the sideband corresponding to resonance with the cavity, and the central peak, are inhibited, while the opposite sideband is enhanced: the larger the Rabi frequency, the more significant the inhibition and enhancement. On the other hand, even if the symmetric three-peak spectrum is considered, when the cavity is tuned to resonance with the atom and the laser field, the ratios of the height and width of the central peak to those of the sidebands are different from the Mollow spectrum in free space. See, for instance, Figs. 10(b) and 10(e).

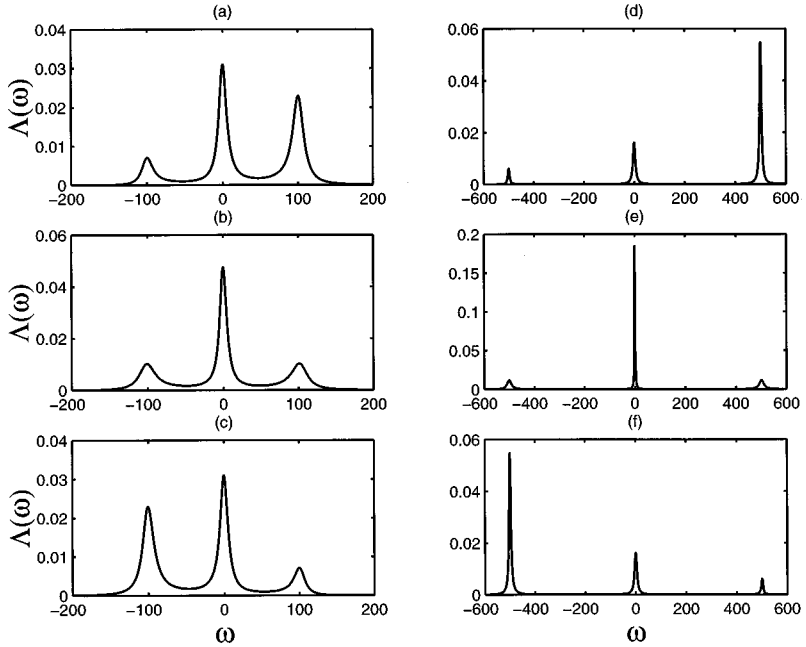

FIG. 10. The incoherent resonance fluorescence spectrum for $\gamma=1$, $g=30$, $\kappa=100$, $\Delta=0$, and different Rabi frequencies $\Omega=100$ in frames (a)–(c), and $\Omega=500$ in frames (d)–(f). The cavity frequency is tuned, respectively, to the lower-frequency sideband ($\delta=-\Omega$) in frames (a) and (d), the center ($\delta=0$) in frames (b) and (e), and the higher-frequency sideband ($\delta=\Omega$) in frames (c) and (f).

The physics associated with the narrowing and asymmetries of the cavity-modified Mollow spectrum can be easily explored by working in the basis of semiclassical dressed states $|\pm\rangle$ [Eq. (31)]. If the condition $\bar{\Omega} \gg \kappa$ holds, the contributions from terms with different resonance frequencies are negligibly small, and the secular approximation is thus valid [3]. The optical Bloch equations then simplify to

$$\begin{aligned} \langle \dot{\Pi}_+ \rangle &= -(\Gamma_\perp - i\bar{\Omega} - i\Omega_{\rm sh})\langle \Pi_+ \rangle, \\ \langle \dot{\Pi}_z \rangle &= -\Gamma_\parallel \langle \Pi_z \rangle + \Gamma_0, \end{aligned} \tag{50}$$

where $\Pi_+ = |+\rangle\langle -|$ is the dressed state transition operator, $\Pi_z = (\Pi_{++} - \Pi_{--})$ with $\Pi_{\pm\pm} = |\pm\rangle\langle\pm|$ being the population operator of the dressed state $|\pm\rangle$, and

$$\begin{aligned} \Gamma_\perp &= \gamma(1 + 2c^2 s^2) + \gamma_c \kappa^2 \left[\frac{4c^2 s^2}{\kappa^2 + \delta^2} + \frac{s^4}{\kappa^2 + (\delta + \bar{\Omega})^2} \right. \\ &\quad \left. + \frac{c^4}{\kappa^2 + (\delta - \bar{\Omega})^2} \right], \\ \Gamma_\parallel &= 2\gamma(c^4 + s^4) + 2\gamma_c \kappa^2 \left[\frac{s^4}{\kappa^2 + (\delta + \bar{\Omega})^2} + \frac{c^4}{\kappa^2 + (\delta - \bar{\Omega})^2} \right], \\ \Gamma_0 &= -2\gamma(c^2 - s^2) + 2\gamma_c \kappa^2 \left[\frac{s^4}{\kappa^2 + (\delta + \bar{\Omega})^2} \right. \\ &\quad \left. - \frac{c^4}{\kappa^2 + (\delta - \bar{\Omega})^2} \right], \\ \Omega_{\rm sh} &= \gamma_c \kappa \left[\frac{s^4(\delta + \bar{\Omega})}{\kappa^2 + (\delta + \bar{\Omega})^2} - \frac{c^4(\delta - \bar{\Omega})}{\kappa^2 + (\delta - \bar{\Omega})^2} \right]. \end{aligned} \tag{51}$$

$\Gamma_\perp$ and $\Gamma_\parallel$ indicate the decay rate of the dressed-state polarization and of the dressed-state population inversion, respectively, while $\Omega_{\rm sh}$ is a frequency shift from the generalized Rabi frequency $\bar{\Omega}$ due to the effects of the intense field and the cavity. All these parameters are resonant when the cavity frequency is tuned to the sidebands of the Mollow spectrum.

The incoherent resonance fluorescence spectrum in the dressed state basis then takes the form

$$\begin{aligned} \Lambda(\omega) &= \frac{4c^2 s^2 \Gamma_\parallel \langle \Pi_{--} \rangle_s \langle \Pi_{++} \rangle_s}{\Gamma_\parallel^2 + \omega^2} + \frac{c^4 \Gamma_\perp \langle \Pi_{++} \rangle_s}{\Gamma_\perp^2 + (\omega - \bar{\Omega} - \Omega_{\rm sh})^2} \\ &\quad + \frac{s^4 \Gamma_\perp \langle \Pi_{--} \rangle_s}{\Gamma_\perp^2 + (\omega + \bar{\Omega} + \Omega_{sh})^2}. \end{aligned} \tag{52}$$

Obviously, the central spectral line with width $2\Gamma_\parallel$ results from the atomic downward transitions between the same dressed states of two adjacent dressed-state doublets, and is proportional to $\langle \Pi_{--} \rangle_s \langle \Pi_{++} \rangle_s$. The left-hand sideband, however, is due to the downward transitions from the substate $|-\rangle$ of one dressed-state doublet to the substate $|+\rangle$ of the next dressed-state doublet, and is associated with the population $\langle \Pi_{--} \rangle_s$ of the dressed state $|-\rangle$. The right-hand sideband originates from the downward transitions $|+\rangle \rightarrow |-\rangle$ between two near-lying dressed-state doublets, and is proportional to $\langle \Pi_{++} \rangle_s$. Both sidebands have the same linewidth $2\Gamma_\perp$.

Here we examine the spectrum for $\Delta = 0$ in detail, as an example of the effect of the cavity resonant frequency on the intense-field resonance fluorescence. We first assume that the cavity is in resonance with the atom and the laser field, $\delta = 0$. Correspondingly, Eq. (51) reduces to

$$\begin{aligned} \Gamma_\perp &= \frac{3\gamma}{2} + \gamma_c \left[1 + \frac{1}{2} \frac{\kappa^2}{\kappa^2 + \Omega^2} \right], \\ \Gamma_\parallel &= \gamma + \gamma_c \frac{\kappa^2}{\kappa^2 + \Omega^2}, \\ \Gamma_0 &= 0. \end{aligned} \tag{53}$$

Therefore, $\langle \Pi_z \rangle_s = \Gamma_0 / \Gamma_\parallel = 0$, that is $\langle \Pi_{++} \rangle_s = \langle \Pi_{--} \rangle_s = \frac{1}{2}$. This leads to a symmetric three-peak spectrum. It is clear that the heights and linewidths of the spectrum are Rabi frequency dependent, which is qualitatively different from the free-space Mollow triplet [1]. All the three spectral lines can be narrowed as the Rabi frequency Ω increases, for example, the central linewidth $2\Gamma_\parallel$ can be reduced from $2(\gamma + \gamma_c)$ to 2γ when Ω increases from $\Omega \ll \kappa$ to $\Omega \gg \kappa$, while the sideband width $2\Gamma_\perp$ can be decreased from $3(\gamma + \gamma_c)$ to $3\gamma + 2\gamma_c$. The ratio of the central peak height to the sideband height is also enlarged from 3 to $3 + 2\gamma_c/\gamma$.

If we tune the cavity frequency to resonance with the Mollow sidebands, $\delta = \pm \bar{\Omega}$, then Eq. (51) gives rise to

$$\begin{aligned} \Gamma_\perp &= \frac{3\gamma}{2} + \gamma_c \left[\frac{1}{4} + \frac{\kappa^2}{\kappa^2 + \Omega^2} + \frac{1}{4} \frac{\kappa^2}{\kappa^2 + 4\Omega^2} \right], \\ \Gamma_\parallel &= \gamma + \frac{\gamma_c}{2} \left[1 + \frac{\kappa^2}{\kappa^2 + 4\Omega^2} \right], \\ \Gamma_0 &= \mp \frac{\gamma_c}{2} \frac{4\Omega^2}{\kappa^2 + 4\bar{\Omega}^2}. \end{aligned} \tag{54}$$

There is thus a population imbalance between the dressed states $|\pm\rangle$, which gives rise to an asymmetric three-peak spectrum. See, for instance, frames (a), (c), (d), and (f) of Fig. 10. In the limit $\Omega \gg \kappa$, the dressed-state population difference is given by

$$\langle \Pi_z \rangle_s \simeq \mp \frac{\gamma_c}{\gamma + \gamma_c}. \tag{55}$$

Hence for the cavity frequency tuned to the lower-frequency sideband of the Mollow fluorescence, $\delta = -\bar{\Omega}$, a dressed-state population inversion ($\langle \Pi_{++} \rangle_s > \langle \Pi_{--} \rangle_s$) is achieved. The heights of the three peaks are straightforwardly deduced to be

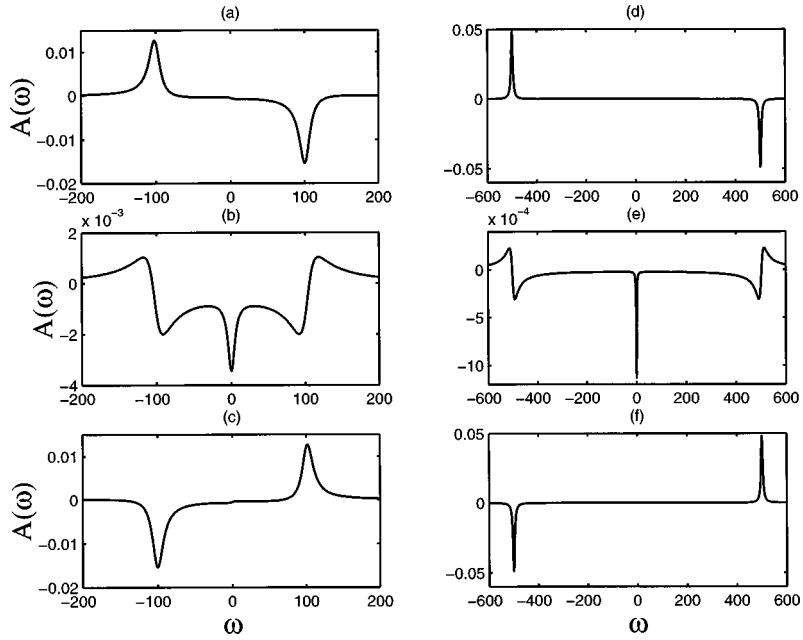

FIG. 11. Same as Fig. 10, but for the probe absorption spectrum.

$$H_{\rm lfs}\simeq\frac{\gamma}{(2\gamma+\gamma_c)(6\gamma+\gamma_c)},$$

$$H_{\rm cen}\simeq\frac{2\gamma(\gamma+\gamma_c)}{(2\gamma+\gamma_c)^3}, \tag{56}$$

$$H_{\rm hfs}\simeq\frac{(\gamma+\gamma_c)}{(2\gamma+\gamma_c)(6\gamma+\gamma_c)}.$$

As expected, the peak of the higher-frequency sideband is enhanced, while the lower-frequency sideband is suppressed.

However, for $\delta=\bar{\Omega}$, that is the cavity is tuned to resonance with the higher-frequency sideband, the population in the state $|-\rangle$ is then greater than that in the state $|+\rangle$. Consequently, the peak of the higher-frequency sideband is lower than that of the lower-frequency sideband. The prediction of the cavity-frequency-dependent asymmetric Mollow triplet is in excellent agreement with the recently experimental observation [16].

On the other hand, the spectrum can be also narrowed as Ω increases. For example, the linewidth of the central peak can be reduced from $2(\gamma+\gamma_c)$ to $2\gamma+\gamma_c$, while the sideband linewidth can be decreased from $3(\gamma+\gamma_c)$ to $3\gamma+\gamma_c/2$ when Ω increases from $\Omega\ll\kappa$ to $\Omega\gg\kappa$. The spectral narrowing is due to the dynamical suppression of the cavity-induced spontaneous emission by the intense field.

VII. ABSORPTION SPECTRUM

The steady-state absorption spectrum of a frequency-tunable very weak probe field is proportional to the Fourier transform of the stationary average value of the two-time commutator of the atomic raising and lowering operators: [4,21,22],

$$A(\omega)=\mathrm{Re}\int_0^\infty\lim_{t\to\infty}\langle[\sigma_-(t),\sigma_+(t+\tau)]\rangle e^{-i\omega\tau}d\tau, \tag{57}$$

where $\omega=\omega_{\rm probe}-\omega_L$ is the frequency of the probe beam measured from the driving laser frequency. Again, invoking the quantum regression theorem together with the optical Bloch equations (40), one can calculate the two-time correlation function $\langle[\sigma_-(\tau),\sigma_+(0)]\rangle$. The absorption spectrum is formally the same as Eq. (46), but with

$$\alpha_1=-\langle\sigma_z\rangle_s,$$

$$\alpha_2=i\langle\sigma_z\rangle_s, \tag{58}$$

$$\alpha_3=\langle\sigma_x\rangle_s-i\langle\sigma_y\rangle_s.$$

We show the probe absorption spectra in Fig. 11, with the parameters. $\gamma=1$, $g=30$, $\kappa=100$, $\Delta=0$, and $\Omega=100$ in frames (a)–(c), and $\Omega=500$ in frames (d)–(f). The cavity frequency is respectively tuned to the lower-frequency sideband of the Mollow triplet ($\delta=-\bar{\Omega}$) in Figs. 11(a) and 11(d), to the center ($\delta=0$) in Figs. 11(b) and 11(e), and to the higher-frequency sideband ($\delta=\bar{\Omega}$) in Figs. 11(c) and 11(f). It is clear from Fig. 11 that when the cavity frequency is tuned to the central line of the Mollow triplet, the central component exhibits a Lorentzian line shape, while the sidebands show a Rayleigh-wing line shape—these profiles are quite similar to the spectral profiles of the probe absorption in free space [4–6]. However, the probe beam is amplified at line center (atomic resonant transition frequency), unlike that in free space where the probe beam is transparent at this frequency. When the cavity is tuned to resonance with one sideband, the center component is negligibly small, and the sidebands exhibit a Lorentzian line shape. The probe beam at one sideband can be amplified, depending on the cavity fre-

quency. Specifically, as the cavity frequency is tuned to the lower-frequency sideband of the Mollow triplet, probe gain is demonstrated at the higher-frequency sideband, otherwise, gain is obtained at the lower-frequency sideband as the cavity frequency is tuned to the higher-frequency sideband of the Mollow triplet. This is also qualitatively different from the absorption spectral features in free space, where the gain at one sideband occurs only when the atom is off resonance with the driving laser field [6].

The probe gain at line center is due to cavity-induced population inversion in the bare-state basis, while the gain at the sidebands stems from the uneven population distribution between the dressed states $|\pm\rangle$. For example, in the case of $\Delta=0$ and $\Omega\gg\kappa$, when the cavity frequency satisfies $\delta=0$, the absorption spectrum can be approximately expressed as

$$A(\omega)\simeq\frac{1}{4}\mathrm{Re}\left[\frac{-2\langle\sigma_z\rangle_s}{\gamma_x+i\omega}+\frac{-i\langle\sigma_y\rangle_s}{(\gamma_y+\gamma_z)/2+i(\omega+\Omega)}+\frac{i\langle\sigma_y\rangle_s}{(\gamma_y+\gamma_z)/2+i(\omega-\Omega)}\right]. \tag{59}$$

Obviously, if $\langle\sigma_z\rangle_s>0$, indicating bare-state population inversion, the central component is then negative—that is, the probe beam is amplified. It is well known that bare-state population inversion can be achieved in such an atom-cavity coupling system for large Rabi frequencies. On the other hand, one finds that the sidebands have Rayleigh-wing line shape, and are associated with the steady-state out-of-phase quadrature of the atomic polarization.

However, when the cavity frequency is tuned to the Mollow sidebands, i.e., $\delta=\pm\Omega$, the absorption spectrum then is given by

$$A(\omega)\simeq\frac{1}{4}\mathrm{Re}\left[\frac{\langle\sigma_x\rangle_s}{(\gamma_y+\gamma_z)/2+i(\omega+\Omega)}+\frac{-\langle\sigma_x\rangle_s}{(\gamma_y+\gamma_z)/2+i(\omega-\Omega)}\right]. \tag{60}$$

In this situation, only the sidebands dominate. Both sidebands show a Lorentzian line shape, and are associated with the steady-state in-phase quadrature of the atomic polarization. In the dressed-state basis, the in-phase quadrature is same as the dressed-state population difference in the case of $\Delta=0$, that is, $\langle\sigma_x\rangle_s=\langle\Pi_z\rangle_s$. It has been shown that when the cavity frequency is tuned to the lower-frequency sideband of the Mollow spectrum, the dressed-state population is inverted, i.e., $\langle\Pi_z\rangle_s>0$, and the resultant absorption spectrum at the higher-frequency sideband has a negative value, showing amplification of the probe beam. Otherwise, if $\delta=\Omega$, then the population in the dressed state $|+\rangle$ is less than that in the dressed state $|-\rangle$, i.e., $\langle\Pi_z\rangle_s<0$; therefore probe gain occurs at the lower-frequency sideband.

VIII. CONCLUSIONS

We have derived a cavity-modified master equation for the atomic density-matrix operator from the full master equation of the composite atom-cavity system, by adiabatically eliminating the cavity variables in the bad cavity limit, which enables us to investigate analytically the dynamical modification of the radiative properties of a strongly driven two-level atom in a single-mode cavity. In particular, we examine the cavity-induced population inversion in the bare-state and dressed-state bases, and the cavity-modified relaxation rates of the phase quadratures of the polarization and the population of the atom, the spectrum of the atomic fluorescence emitted out the side of the cavity, and the probe absorption spectrum. We find that all these quantities are very sensitive to the atom-cavity coupling, Rabi frequency, and cavity resonant frequency.

More specifically, atomic population inversion in the bare-state basis as well as in the dressed-state basis can be achieved for appropriate atom-cavity coupling constants and cavity resonant frequency and high driving intensities. Population inversion is impossible in free space. We also gain physical insight into the cavity-induced population inversion both in the bare- and dressed-state representations by performing an analysis in terms of rate equations, which allow one to examine the modifications of the atomic population transfer rates. The bare-state population inversion results from the enhancement of the stimulated absorption rate and the simultaneous inhibition of the stimulated emission by the atom-cavity coupling. The dressed-state population inversion is due to the enhanced atom-cavity interaction when the cavity is tuned to resonance with the atomic dressed-state transition. When the cavity is tuned to resonance with the center of the Mollow fluorescence triplet, the cavity-induced decay rate (into the cavity mode) of the in-phase quadrature of the atomic polarization can be greatly suppressed, and the incoherent resonance fluorescence spectrum shows a symmetric three-peaked structure with Rabi-frequency-dependent linewidths and heights, while the absorption spectrum also has three symmetric components, but with probe gain at line center. However, when the cavity frequency is tuned to one Mollow sideband, the cavity-induced relaxation rate of the out-of-phase quadrature can be largely suppressed, and both spectra are asymmetric. For the resonance fluorescence spectrum the central peak and the sideband on resonance with the cavity are significantly reduced, while the sideband far-off resonance with the cavity is enhanced. Probe gain may occur at the far-off resonance sideband. In all situations, the sidebands of the fluorescence and absorption spectra are shifted slightly from the standard Mollow sideband position. All the spectral lines can be narrowed by increasing the driving intensity. The physics of these striking spectral features is interpreted in the dressed-state basis. We also briefly discussed our theoretical predictions in the context of the experimental observations of the cavity-modified resonance fluorescence of a strongly driven two-level atom [15,16].

ACKNOWLEDGMENTS

This work was supported by the United Kingdom EPSRC, by the EC, and by NATO.

[1] B. R. Mollow, Phys. Rev. **188**, 1969 (1969); F. Y. Wu, R. E. Grove, and S. Ezekiel, Phys. Rev. Lett. **35**, 1426 (1977).

[2] For reviews, see, for example, S. Swain, Adv. At. Mol. Phys. **16**, 159 (1980); B. R. Mollow, Prog. Opt. **XIX**, 1 (1981); in *Dissipative Systems in Quantum Optics*, edited by R. Bonifacio (Springer, Berlin, 1982); J. D. Cresser, J. Hager, G. Leuchs, M. Rateike, and H. Walther, in *Dissipative Systems in Quantum Optics*, edited by R. Bonifacio (Springer, Berlin, 1982).

[3] C. Cohen-Tannoudji and S. Reynaud, in *Multiphoton Processes*, edited by J. H. Eberly and P. Lambropoulos (Wiley, New York, 1978); J. Phys. **10**, 345 (1977); C. Cohen-Tannoudji, J. Dupont-Roc, and G. Grynberg, *Atom-Photon Interactions* (Wiley, New York, 1992).

[4] B. R. Mollow, Phys. Rev. A **5**, 2217 (1972); F. Y. Wu, S. Ezekiel, M. Ducloy, and B. R. Mollow, Phys. Rev. Lett. **38**, 1077 (1977).

[5] M. Sargent III, Phys. Rep. **43**, 223 (1978); G. S. Agarwal, Phys. Rev. A **19**, 923 (1979); R. W. Boyd, M. G. Raymer, P. Narum, and D. J. Harter, *ibid.* **24**, 411 (1981); P. Meystre and M. Sargent III, *Elements of Quantum Optics* (Springer-Verlag, Berlin, 1991).

[6] G Khitrova, P. R. Berman, and M. Sargent III, J. Opt. Soc. Am. B **5**, 160 (1988); G. Grynberg and C. Cohen-Tannoudji, Opt. Commun. **96**, 150 (1993); H. Y. Ling and S. Barbay, *ibid.* **111**, 350 (1994); C. Szymanowski, C. H. Keitel, B. J. Dalton, and P. L. Knight, J. Mod. Opt. **42**, 985 (1995).

[7] For recent reviews, see, for example, *Cavity Quantum Electrodynamics*, edited by P. R. Berman, (Academic, London, 1994); S. Haroche, in *Fundamental Systems in Quantum Optics Les Houches, Session LIII*, edited by J. Dalbard, J. M. Raimond, and J. Zinn-Justin (Elsevier, Amsterdam, 1992).

[8] E. M. Purcell, Phys. Rev. **69**, 681 (1946); P. Goy, J. M. Raimond, M. Gross, and S. Haroche, Phys. Rev. Lett. **50**, 1903 (1983); D. J. Heinzen and M. S. Feld, *ibid.* **59**, 2623 (1987); F. De Martini and G. R. Jacobovitz, *ibid.* **60**, 1711 (1988).

[9] D Kleppner, Phys. Rev. Lett. **47**, 233 (1981); D. P. O'Brien, P. Meystre, and H. Walther, Adv. At. Mol. Phys. **21**, 1 (1985); R. G. Hulet, E. S. Hilfer, and D. Kleppner, Phys. Rev. Lett. **55**, 2137 (1985); W. Jhe, A. Anderson, E. A. Hinds, D. Meschede, L. Moi, and S. Haroche, *ibid.* **58**, 666 (1987); D. J. Heinzen, J. J. Childs, J. E. Thomas, and M. S. Feld, *ibid.* **58**, 1320 (1987).

[10] J. J. Sanchez-Mondragon, N. G. Narozhny, and J. H. Eberly, Phys. Rev. Lett. **51**, 550 (1983); G. S. Agarwal, *ibid.* **53**, 1732 (1984); M. G. Raizen, R. J. Thompson, R. J. Brecha, H. J. Kimble, and H. J. Carmichael, *ibid.* **63**, 240 (1989); R. J. Thompson, G. Rempe, and H. J. Kimble, *ibid.* **68**, 1132 (1992); F. Bernadot, P. Nussenzveig, M. Brune, J. M. Raimond, and S. Haroche, Europhys. Lett. **17**, 33 (1992).

[11] P. R. Rice and H. J. Carmichael, IEEE J. Quantum Electron. **24**, 1351 (1988). For extension to a cavity damped by a squeezed vacuum, see, for example, P. R. Rice and L. M. Pedrotti, J. Opt. Soc. Am. B **9**, 2008 (1992); J. I. Cirac, Phys. Rev. A **46**, 4354 (1992); W. S. Smyth and S. Swain, *ibid.* **53**, 2846 (1996); P. Zhou and S. Swain, Opt. Commun. **131**, 153 (1996).

[12] C. M. Savage, Phys. Rev. Lett. **60**, 1828 (1988); M. Lindberg and C. M. Savage, Phys. Rev. A **38**, 5182 (1988).

[13] M. Lewenstein, T. W. Mossberg, and R. J. Glauber, Phys. Rev. Lett. **59**, 775 (1987); M. Lewenstein and T. W. Mossberg, Phys. Rev. A **37**, 2048 (1988).

[14] W. Lange and H. Walther, Phys. Rev. A **48**, 4551 (1993); G. S. Agarwal, W. Lange, and H. Walther, *ibid.* **48**, 4555 (1993).

[15] Y. Zhu, A. Lezama, and T. W. Mossberg, Phys. Rev. Lett. **61**, 1946 (1988).

[16] A. Lezama, Y. Zhu, S. Morin, and T. W. Mossberg, Phys. Rev. A **39**, R2754 (1989).

[17] C. M. Savage, Phys. Rev. Lett. **63**, 1376 (1989); Quantum Opt. **2**, 89 (1990).

[18] J. I. Cirac, H. Ritsch, and P. Zoller, Phys. Rev. A **44**, 4541 (1991).

[19] M. Loffler, G. M. Meyer, and H. Walther, Phys. Rev. A **55**, 3923 (1997).

[20] T. Quang and H. Freedhoff, Phys. Rev. A **47**, 2285 (1993).

[21] H. Freedhoff and T. Quang, Phys. Rev. Lett. **72**, 474 (1994).

[22] H. Freedhoff and T. Quang, J. Opt. Soc. Am. B **10**, 1337 (1993); **12**, 9 (1995).

[23] C. W. Gardiner, Phys. Rev. Lett. **56**, 1917 (1986).

[24] E. T. Jaynes and F. W. Cummings, Proc. IEEE **51**, 89 (1963); H. J. Carmichael, in *Atomic and Molecular Physics and Quantum Optics*, edited by H. A. Bachor, K. Kumar, and B. A. Robson (World Scientific, Singapore, 1992), and references therein.

[25] S. M. Barnett and P. L. Knight, Phys. Rev. A **33**, 2444 (1986).

[26] J. I. Cirac, Phys. Rev. A **46**, 4354 (1992).